Design, synthesis and biological evaluation of colchicine derivatives as novel tubulin and histone deacetylase dual inhibitors

ARTICLE *in* EUROPEAN JOURNAL OF MEDICINAL CHEMISTRY · MAY 2015

Impact Factor: 3.45 · DOI: 10.1016/j.ejmech.2015.03.035

European Journal of Medicinal Chemistry 95 (2015) 127–135

Contents lists available at ScienceDirect

European Journal of Medicinal Chemistry

journal homepage: http://www.elsevier.com/locate/ejmech

Original article

Design, synthesis and biological evaluation of colchicine derivatives as novel tubulin and histone deacetylase dual inhibitors

Xuan Zhang [a], Yannan Kong [b], Jie Zhang [c], Mingbo Su [d], Yubo Zhou [d], Yi Zang [d], Jia Li [d], Yi Chen [c], Yanfen Fang [b, *], Xiongwen Zhang [b], Wei Lu [a, *]

[a] Institute of Drug Discovery and Development, East China Normal University, Shanghai 200062, PR China
[b] Shanghai Engineering Research Center of Molecular Therapeutics and New Drug Development, East China Normal University, Shanghai 200062, PR China
[c] State Key Laboratory of Drug Research, Shanghai Institute of Materia Medica, Chinese Academy of Sciences, Shanghai 201203, PR China
[d] National Center for Drug Screening, State Key Laboratory of Drug Research, Shanghai Institute of Materia Medica, Chinese Academy of Sciences, Shanghai 201203, PR China

ARTICLE INFO

Article history:
Received 11 January 2015
Received in revised form
14 March 2015
Accepted 17 March 2015
Available online 18 March 2015

Keywords:
Colchicine
Dual inhibitor
HDAC
Tubulin
Hybrid

ABSTRACT

A new class of colchicine derivatives were designed and synthesized as tubulin–HDAC dual inhibitors. Biological evaluations of these hybrids included the inhibitory activity of HDAC, tubulin polymerization analysis, *in vitro* cell cycle analysis in HCT-116 cells and cytotoxicity against different cancer cell lines. Hybrid **6d** behaved as potent HDAC–tubulin dual inhibitor and showed comparable cytotoxicity with colchicine. Compound **11a** exhibited powerful tubulin inhibitory activity, moderate anti-HDAC activity and the most potent cytotoxicity (IC_{50} = 2–105 nM).

1. Introduction

Though cancer pharmacotherapy has a long history of more than 70 years, it is still a great challenge to cure cancer. In 2012, there were more than 14 million new cancer cases around the world and the number is expected to continuously increase in the next 20 years [1]. Traditional antitumor drugs including cytotoxic agents have been widely used for years. However, the usage of these drugs is hindered by severe toxicity and other undesirable side effects. The development of targeted molecularly anti-cancer drugs has made significant achievement over the past decade. But only part patients show positive response. In addition, the acquired drug resistance may limit the use of these agents. As a matter of fact, diseases with linear pathways might be well treated with single target agents. However, cancer is a disease with complex signaling networks, which means it is difficult to treat most cancers by using single classical targeted drug [2]. Combination chemotherapy can simultaneously block several key signaling pathways and create synergistic antitumor effects [3–11]. These regimens are widely used and can improve therapeutic efficacy and reduce drug toxicity.

Recently, multi-target drug design has become an active research field [12–14]. These agents can create synergistic anti-cancer effects. Compared with combination chemotherapy, they always exhibit simpler pharmacokinetics. Histone deacetylase (HDAC) involved multi-target drug design is one of the hotspots in this area. HDAC plays an important role in the regulation of gene expression. HDAC inhibitors can cause growth arrest, differentiation and apoptosis in cancer cells [15–18]. In general, a HDAC inhibitor consists of a capping group, a zinc-binding group (ZBG) and an appropriate linker (Fig. 1). The effectiveness in oncotherapy together with the simple SAR has attracted many oncologists into the exploration of HDAC-involved multi-target agents [19–26].

Three HDAC-targeting drugs, vorinostat (SAHA), romidepsin and belinostat have been approved by FDA for the treatment of cutaneous T-cell lymphoma and peripheral T-cell lymphoma [27–30]. Over 12 HDAC inhibitors are currently in clinical trials for different cancers [31,32]. Zinc-binding groups play an important role in the binding efficiency between HDAC inhibitors and enzyme. Among

* Corresponding authors.
E-mail addresses: yffang@sat.ecnu.edu.cn (Y. Fang), wlu@chem.ecnu.edu.cn (W. Lu).

http://dx.doi.org/10.1016/j.ejmech.2015.03.035
0223-5234/

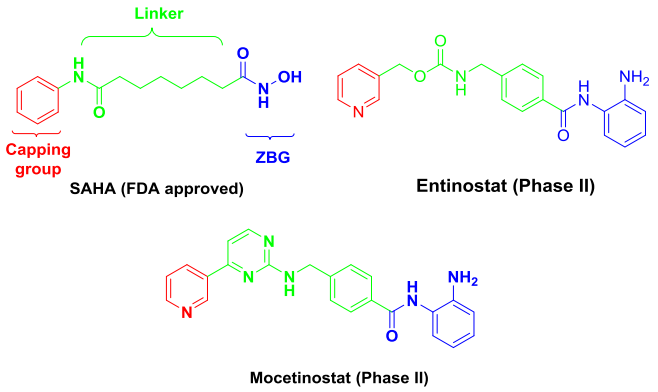

Fig. 1. Representative structures of HDAC inhibitors.

all types of ZBGs, hydroxamate and benzamide are most widely studied [23].

Previously, we reported a series of colchicine–SAHA hybrids as novel antitumor agents based on the synergistic antitumor effect between HDAC inhibitors and tubulin inhibitors [25,33–35]. Among these hybrids, compound **1** behaved as tubulin–HDAC dual inhibitor and displayed the best *in vitro* antiproliferative activity. This work suggested that the colchicine moiety is an appropriate capping group for HDAC inhibitors. For HDAC-involved dual inhibitors, ZBG might contribute to the binding activities of both targets. To further explore this kind of tubulin–HDAC dual inhibitors, we designed and synthesized a new series of colchicine derivatives with benzamide moiety as HDAC ZBG (Fig. 2). The biological evaluations of these molecules include the inhibitory activity of HDAC, tubulin polymerization analysis, *in vitro* cell cycle analysis in HCT-116 cells and cytotoxicity against different cancer cell lines.

2. Results and discussion

2.1. Chemistry

The general route for the synthesis of colchicine derivatives with amide linkage is depicted in Scheme 1. The benzoic acid **2** or **3** was treated with $SOCl_2$ followed by the corresponding amines in the presence of triethylamine to afford compounds **4a**–**d**. Hydrolysis of these esters with LiOH gave the corresponding carboxylic acids. Subsequent amidation of these intermediates with de-Ac-colchicine [36,37] afforded compounds **5a**–**d**. Finally, treatment of these compounds with TFA gave the target molecules **6a**–**d**.

As shown in Scheme 2, preparation of dual inhibitors with amine linkage started from hydroxymethyl benzoic acids **7** or **8**. These acids were treated with $SOCl_2$ followed by the corresponding amines in the presence of triethylamine to give compounds **9a**–**d** in good yields. Subsequently, these molecules were treated with de-Ac-colchicine to afford compounds **10a**–**d**. Target hybrids **11a**–**d** were obtained after the removal of protecting groups.

2.2. Functional assay

2.2.1. In vitro HDAC inhibitory activity

We first tested the HDAC inhibition activity of the hybrids against recombinant human HDAC1, HDAC2 and HDAC3 enzymes, using mocetinostat as the positive control compound. As shown in Table 1, all of the hybrids exhibited inhibitory activity against HDAC1, HDAC2 and HDAC3 except compound **11c**. The ZBG type had a great influence on anti-HDAC activity. Compared with hybrids equipped with unsubstituted benzamide ZBG, their analogs with bis(aryl)-type ZBG showed better potency against HDAC1-3, which was consistent with the reported literature (**6a** vs **6b**, **6c** vs **6d**, **11a** vs **11b** and **11c** vs **11d**) [38]. Among these conjugates, compound **6d** showed the most potent anti-HDAC activity against HDAC1 (IC_{50} = 1.50 μM), HDAC2 (IC_{50} = 0.19 μM) and HDAC3 (IC_{50} = 1.49 μM).

2.2.2. Effect of hybrids on the tubulin polymerization

To probe the impact of these hybrids on tubulin polymerization dynamics, we followed the kinetics of tubulin polymerization in the presence of colchicine and hybrids. As shown in Fig. 3, colchicine can block the polymerization of tubulin into microtubules while mocetinostat had very little effect [39]. Most of the hybrids caused inhibition on tubulin polymerization when compared to control group. Among these tested molecules, compounds **6d**, **11a** and **11c** displayed comparable tubulin inhibitory activity with the positive control colchicine.

2.2.3. Effect of compounds *6d* and *11a* on cell cycle

Cell cycle analysis of the best HDAC inhibitor **6d** and the most powerful tubulin polymerization inhibitor **11a** was investigated. Fig. 4 shows a significantly increased G_2/M peak after treatment of HCT-116 cells with colchicine at 20 nM. In consistence with the tubulin polymerization inhibition effects, **6d** and **11a** have also exhibited the cell cycle arrest effects. Compared with colchicine, cells treated with **6d** or **11a** at 10 nM has already showed a striking G_2/M phase arrest.

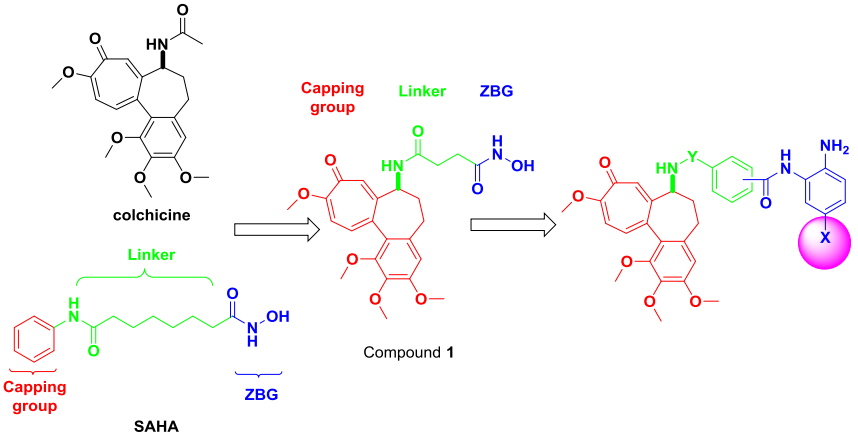

Fig. 2. Design of novel tubulin-HDAC dual inhibitors.

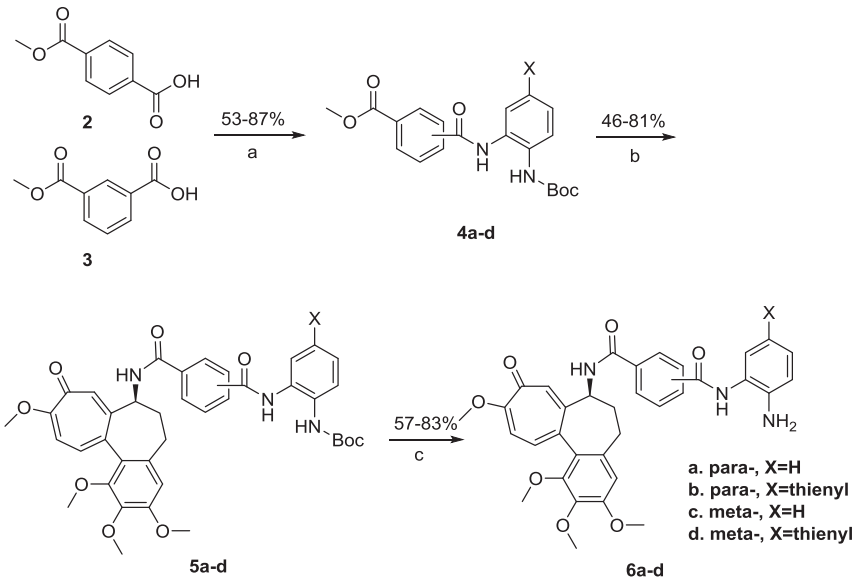

Scheme 1. Synthesis of tubulin-HDAC dual inhibitors with amide linkage. Reagents and conditions: a) i. $SOCl_2$, toluene, 60 °C; ii. triethylamine, DCM; b) i. LiOH, MeOH, H_2O; ii. de-Ac-colchicine, HATU, triethylamine, DCM; c) TFA, DCM.

2.2.4. In vitro anticancer activity

Evaluation of the antiproliferative activity of designed hybrids on A549 human lung adenocarcinoma cell line was performed using the MTT assay. As shown in Table 2, all of the conjugates can cause cell growth inhibition and showed submicromolar-micromolar IC_{50} values. Compound **11a** showed the best cytotoxicity which is comparable with colchicine (IC_{50} = 0.106 μM). Surprisingly, compound **6d** with powerful HDAC and tubulin inhibitory activity displayed moderate antiproliferative activity against A549 cell line (IC_{50} = 2.790 μM). The difference between their cytotoxicity could be due to the different cell membrane penetration.

Subsequently, we selected compounds **6d** and **11a** to evaluate their antiproliferative activity against a panel of human cancer cell lines including colorectal cancer (HCT-116, SW620), hepatocellular carcinoma (Hep3B, HeoG2 and MHCC97H), gastric cancer (SNU-5, SNU-16 AND MKN-45), pancreatic carcinoma (PANC-1) and osteosarcoma (SJSA-1). As shown in Table 3, HDAC inhibitor mocetinostat showed moderate cytotoxicity while tubulin inhibitor colchicine displayed excellent growth inhibitory activity against these cancer cells. The antiproliferative activity of dual inhibitor **6d** is comparable with colchicine. Hybrid **11a** showed improved cytotoxicity toward most of tested cancer cell lines. Especially on HCT-116 cells, the growth inhibitory activity is 8- fold more potent than the parent compound colchicine.

3. Conclusion

In conclusion, as a continuation of our previous work, we prepared a new series of colchicine derivatives. Benzamide type HDAC zinc binding group was introduced into designed hybrids to regulate HDAC and tubulin inhibitory activity. Biological evaluation displayed that most of these hybrids with colchicine moiety as HDAC capping group exhibited potent HDAC inhibitory activity.

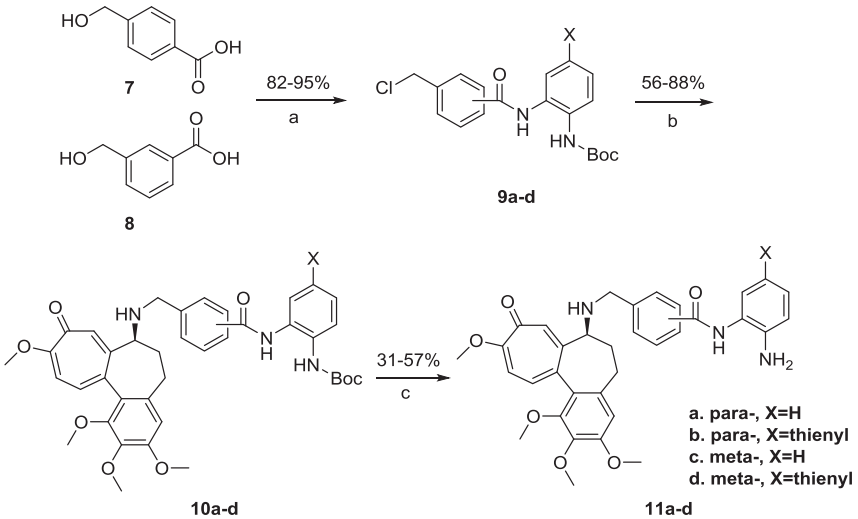

Scheme 2. Synthesis of tubulin-HDAC dual inhibitors with amine linkage. Reagents and conditions: a) i. $SOCl_2$, toluene, 60 °C; ii. triethylamine, DCM; b) de-Ac-colchicine, NaOAc, KI, THF, reflux; c) TFA, DCM.

Table 1
In vitro HDAC Inhibition.[a]

Compound	IC_{50} (μM) ± SD[a]		
	HDAC1	HDAC2	HDAC3
Mocetinostat	0.39 ± 0.03	0.17 ± 0.00	0.36 ± 0.00
Colchicine	-[b]	–	–
6a	15.92 ± 2.62	10.42 ± 0.20	12.10 ± 2.40
6b	2.24 ± 0.08	0.38 ± 0.00	1.97 ± 0.08
6c	9.62 ± 1.49	4.91 ± 0.31	10.78 ± 1.16
6d	1.50 ± 0.36	0.19 ± 0.00	1.49 ± 0.13
11a	12.50 ± 1.13	6.73 ± 0.25	11.23 ± 0.46
11b	3.32 ± 0.71	0.27 ± 0.03	1.47 ± 0.06
11c	–	–	–
11d	25.50 ± 1.49	5.41 ± 0.28	19.68 ± 2.02

[a] Each value was reproduced in three experiments.
[b] IC_{50} > 20 μg/mL.

Compared with molecules equipped with unsubstituted benzamide ZBG, hybrids with bis(aryl)-type ZBG showed better anti-HDAC activity. Compound **6d** displayed the most efficient anti-HDAC activity which is comparable with mocetinostat. On the other hand, though it is difficult to conclude the SAR for their tubulin inhibitory activity, the introduction of HDAC pharmacophore into colchicine core kept its anti-tubulin activity. Compounds **6d**, **11a** and **11c** displayed similar anti-tubulin activity with colchicine. Potent HADC–tubulin dual inhibitor **6d** exhibited comparable *in vitro* antiproliferative activity with colchicine. Compound **11a** with powerful tubulin inhibitory activity and moderate anti-HDAC activity showed superior cytotoxicity to the positive control compound (IC_{50} = 2–105 nM). The present inspiriting results give a promising future for the optimization of the series. This finding could be of interest in the search for efficient anticancer multi-target agents.

4. Experimentals

4.1. General

Melting points were taken on a Fisher–Johns melting point apparatus, uncorrected and reported in degrees Centigrade. ^{1}H NMR spectra and ^{13}C NMR were recorded in $CDCl_3$ and DMSO-d_6 on a Bruker DRX-400 (400 MHz) using TMS as internal standard.

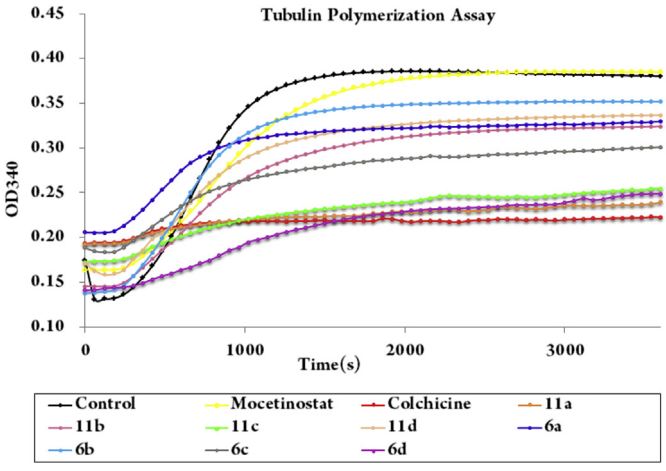

Fig. 3. Kinetics of tubulin polymerization in the absence and presence of 10 μM solution of hybrids. Tubulin (4.0 mg/mL) was polymerized in the absence and presence of 10 μM of colchicine and each of hybrids. The change in absorbance at 340 nm was monitored.

Chemical shifts were reported as δ (ppm) and spin–spin coupling constants as *J* (Hz) values. The mass spectra (MS) were recorded on a Finnigan MAT-95 mass spectrometer. The purity of all tested compounds was established by HPLC to be >95.0%. HPLC analysis was performed at room temperature using an Agilent Eclipse XDB-C18 (250 mm × 4.6 mm) and as a mobile phase gradient from 10% MeOH/H_2O (1‰ AcOH) for 1 min, 10% MeOH/H_2O (1‰ AcOH) to 60% MeOH/H_2O (1‰ AcOH) for 6 min, 60% MeOH/H_2O (1‰ AcOH) to 90% MeOH/H_2O (1‰ AcOH) for 6 min and 90% MeOH/H_2O (1‰ AcOH) for 5 min more, a flow rate of 1.0 mL/min and plotted at 254 nm.

4.2. Representative procedure for ***4a–d***

Acid **2**/**3** (1.0 equiv), $SOCl_2$ (6.0 equiv) and DMF (1 drop) were stirred in toluene at 60 °C for 2 h. Then the solvent was removed under reduced pressure. The acyl chloride was dissolved in DCM and added dropwise into a solution of corresponding aromatic amine (1.0 equiv) and triethylamine (2.0 equiv). After the addition, the mixture was stirred at room temperature for 1 h and extracted with EtOAc. The organic layer was washed with 1 N HCl (aq) followed by 10% Na_2CO_3 (aq) and dried over Na_2SO_4. Concentrated in vacuo gave the crude product, which was further purified by crystallization from EtOAc-light petroleum.

4.2.1. Methyl 4-((2-((tert-butoxycarbonyl)amino)phenyl) carbamoyl)benzoate (***4a***)

Starting from acid **2** and tert-butyl (2-aminophenyl)carbamate, 87% of compound **4a** was obtained as white solid. mp 142–143 °C, ^{1}H NMR (400 MHz, *d6*-DMSO) δ 9.98 (s, 1H), 8.71 (s, 1H), 8.15–8.03 (m, 4H), 7.55 (dd, *J* = 13.6, 7.8 Hz, 2H), 7.27–7.08 (m, 2H), 3.91 (s, 3H), 1.44 (s, 9H); HRMS (ESI): *m/z* calcd for $C_{20}H_{22}N_2NaO_5$ ($M + Na^+$): 393.1421, found: 393.1412.

4.2.2. Methyl 4-((2-((tert-butoxycarbonyl)amino)-5-(thiophen-2-yl)phenyl)carbamoyl)benzoate (***4b***)

Starting from acid **2** and tert-butyl (2-amino-4-(thiophen-2-yl) phenyl)carbamate, 75% of compound **4a** was obtained as pale yellow solid. mp 206–208 °C, ^{1}H NMR (400 MHz, *d6*-DMSO) δ 10.07 (s, 1H), 8.77 (s, 1H), 8.22–8.08 (m, 4H), 7.81 (d, *J* = 1.7 Hz, 1H), 7.65 (d, *J* = 8.5 Hz, 1H), 7.58–7.50 (m, 2H), 7.46 (d, *J* = 3.1 Hz, 1H), 7.13 (dd, *J* = 5.0, 3.7 Hz, 1H), 3.90 (d, *J* = 9.4 Hz, 3H), 1.45 (s, 9H); HRMS (ESI): *m/z* calcd for $C_{24}H_{24}N_2NaO_5S$ ($M + Na^+$): 475.1298, found: 475.1297.

4.2.3. Methyl 3-((2-((tert-butoxycarbonyl)amino)phenyl) carbamoyl)benzoate (***4c***)

Starting from acid **3** and tert-butyl (2-aminophenyl)carbamate, 53% of compound **4a** was obtained as white solid. mp 129–130 °C, ^{1}H NMR (400 MHz, $CDCl_3$) δ 9.36 (s, 1H), 8.62 (s, 1H), 8.31–8.08 (m, 2H), 7.76 (d, *J* = 7.6 Hz, 1H), 7.56 (t, *J* = 7.7 Hz, 1H), 7.26–7.09 (m, 3H), 6.86 (s, 1H), 3.95 (s, 3H), 1.50 (s, 9H); HRMS (ESI): *m/z* calcd for $C_{20}H_{22}N_2NaO_5$ ($M + Na^+$): 393.1421, found: 393.1421.

4.2.4. Methyl 3-((2-((tert-butoxycarbonyl)amino)-5-(thiophen-2-yl)phenyl)carbamoyl)benzoate (***4d***)

Starting from acid **3** and tert-butyl (2-amino-4-(thiophen-2-yl) phenyl)carbamate, 59% of compound **4a** was obtained as pale yellow solid. mp 142–144 °C, ^{1}H NMR (400 MHz, $CDCl_3$) δ 9.29 (br s, 1H), 8.65 (s, 1H), 8.22 (dd, *J* = 13.6, 7.8 Hz, 2H), 8.09 (d, *J* = 1.6 Hz, 1H), 7.58 (t, *J* = 7.7 Hz, 1H), 7.43 (dd, *J* = 8.3, 2.1 Hz, 1H), 7.33–7.26 (m, 3H), 7.07 (dd, *J* = 5.1, 3.6 Hz, 1H), 6.75 (s, 1H), 3.96 (s, 3H), 1.52 (s, 9H); HRMS (ESI): *m/z* calcd for $C_{24}H_{24}N_2NaO_5S$ ($M + Na^+$): 475.1298, found: 475.1300.

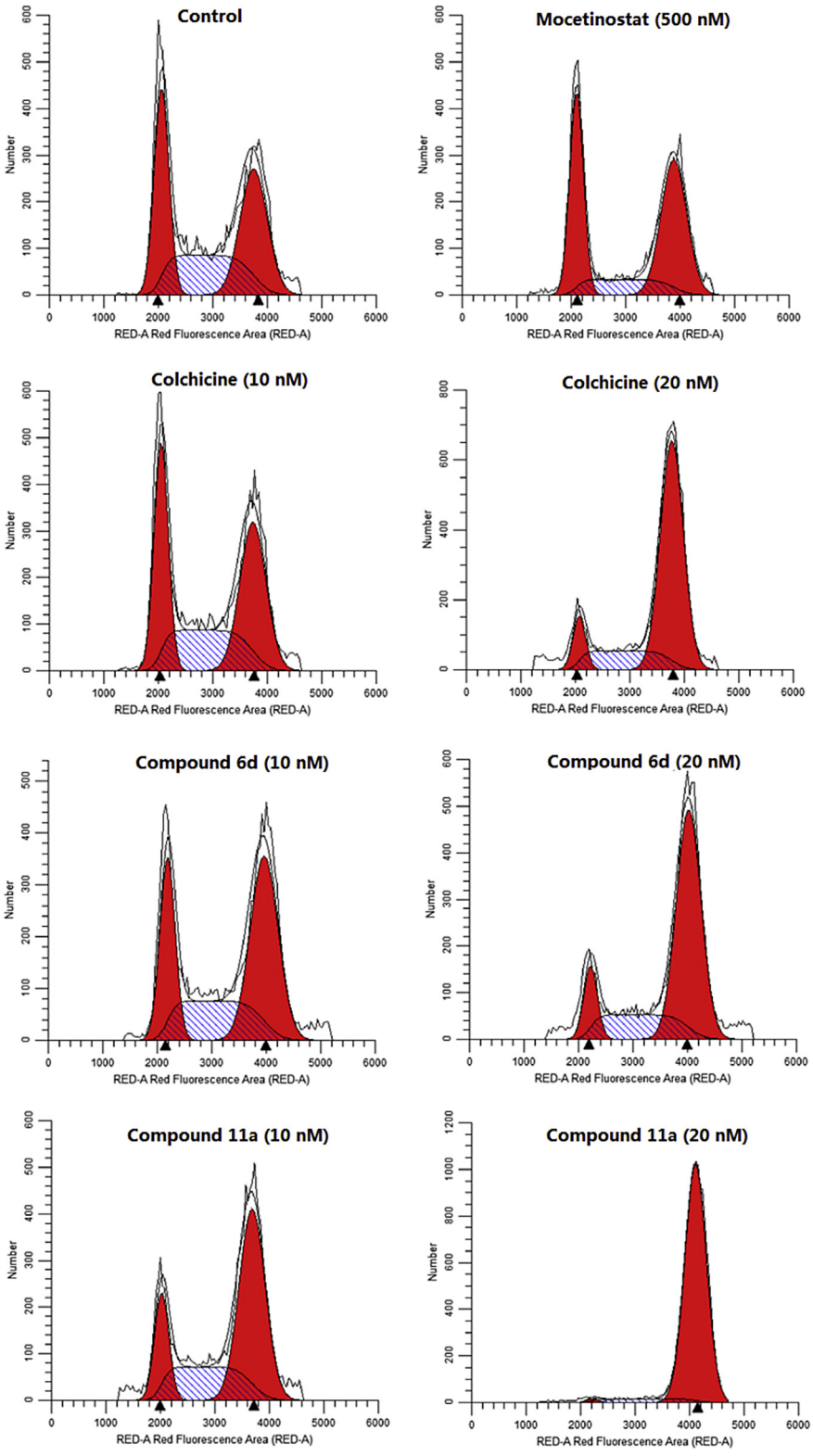

Fig. 4. Effect of hybrids **6d** and **11a** on cell cycle. Colchicine was used as a positive control.

4.3. *Representative procedure for **5a–d***

Ester (1.0 equiv) and LiOH (2.0 equiv) were stirred in a solution of MeOH and H_2O for 3 h at room temperature. Then 1 N HCl (aq) (2.2 equiv) was added into the flask and the mixture was concentrated in vacuo. The crude acid (1.0 equiv), de-Ac-colchicine (0.83 equiv), DIPEA (2.5 equiv) and HATU (0.87 equiv) were stirred in DCM for 2 h. Subsequently, the mixture was extracted with DCM, washed with 1 N HCl (aq), dried over Na_2SO_4 and concentrated in vacuo. The crude product was further purified by column

Table 2
In vitro Cell Growth Inhibition against A549 cell line.[a]

Compound	A549	Compound	A549
Colchicine	0.105	**Mocetinostat**	2.080
6a	1.620	**11a**	0.106
6b	0.740	**11b**	1.040
6c	3.430	**11c**	0.354
6d	2.790	**11d**	0.393

[a] Each value was reproduced in three experiments.

Table 3
Evaluation of compounds **6d** and **11a** against a panel of human cancer cell lines.[a]

Cell line	Mocetinostat (μM)	Colchicine (μM)	**6d** (μM)	**11a** (μM)
HCT-116	0.396	0.040	0.039	0.005
SW620	0.419	0.005	0.004	0.002
Hep3B	0.823	0.014	0.010	0.005
HepG2	0.876	0.027	0.020	0.014
MHCC97H	4.563	0.110	0.339	0.043
SNU-5	1.009	0.034	0.119	0.014
SNU-16	0.142	0.005	0.005	0.002
MKN-45	0.610	0.002	0.002	0.002
PANC-1	26.774	0.021	0.019	0.005
SJSA-1	3.624	0.008	0.027	0.009

[a] Each value was reproduced in three experiments.

chromatography (DCM: MeOH = 20:1).

4.3.1. Compound ***5a***

Starting from acid **4a**, 81% of compound **5a** was obtained as pale yellow solid. mp 184–186 °C, ^{1}H NMR (400 MHz, $CDCl_3$) δ 9.38 (s, 1H), 7.84–7.67 (m, 6H), 7.63 (s, 1H), 7.41–7.35 (m, 2H), 7.23–7.13 (m, 3H), 6.90 (d, J = 10.9 Hz, 1H), 6.58 (s, 1H), 4.97–4.81 (m, 1H), 4.00 (d, J = 12.6 Hz, 3H), 3.98–3.87 (m, 6H), 3.61 (s, 3H), 2.68–2.55 (m, 1H), 2.53–2.31 (m, 2H), 2.20–2.06 (m, 1H), 1.45 (s, 9H); HRMS (ESI): m/z calcd for $C_{39}H_{41}N_3O_9Na$ (M + Na^+): 718.2735, found: 718.2750.

4.3.2. Compound ***5b***

Starting from acid **4b**, 50% of compound **5b** was obtained as pale yellow solid. mp 188–190 °C, ^{1}H NMR (400 MHz, $CDCl_3$) δ 9.41 (s, 1H), 7.99 (s, 1H), 7.83–7.71 (m, 5H), 7.53 (s, 1H), 7.40–7.31 (m, 4H), 7.26–7.22 (m, 2H), 7.07–7.04 (m, 1H), 6.90 (d, J = 11.0 Hz, 1H), 6.53 (s, 1H), 4.90–4.78 (m, 1H), 4.02 (s, 3H), 3.93–3.89 (m, 6H), 3.64 (s, 3H), 2.53–2.29 (m, 3H), 2.08–2.01 (m, 1H), 1.46 (s, 9H); HRMS (ESI): m/z calcd for $C_{43}H_{43}N_3O_9SNa$ (M + Na^+): 800.2612, found: 800.2606.

4.3.3. Compound ***5c***

Starting from acid **4c**, 46% of compound **5c** was obtained as yellow solid. 176–178 °C, ^{1}H NMR (400 MHz, $CDCl_3$) δ 9.20 (br s, 1H), 8.51 (br s, 1H), 8.12 (br s, 1H), 7.98 (t, J = 7.4 Hz, 2H), 7.67 (s, 1H), 7.57 (d, J = 8.1 Hz, 1H), 7.50–7.31 (m, 4H), 7.21 (t, J = 7.1 Hz, 1H), 7.11 (t, J = 7.1 Hz, 1H), 6.82 (d, J = 11.0 Hz, 1H), 6.54 (s, 1H), 4.87–4.74 (m, 1H), 3.94 (s, 3H), 3.90 (s, 3H), 3.86 (s, 3H), 3.68 (s, 3H), 2.59–2.50 (m, 1H), 2.46–2.33 (m, 2H), 2.03–1.84 (m, 1H), 1.43 (s, 9H); HRMS (ESI): m/z calcd for $C_{39}H_{41}N_3O_9Na$ (M + Na^+): 718.2735, found: 718.2746.

4.3.4. Compound ***5d***

Starting from acid **4d**, 68% of compound **5d** was obtained as yellow solid. 182–183 °C, ^{1}H NMR (400 MHz, $CDCl_3$) δ 9.20 (br s, 1H), 8.51 (br s, 1H), 8.12 (br s, 1H), 7.98 (t, J = 7.4 Hz, 2H), 7.67 (s, 1H), 7.57 (d, J = 8.1 Hz, 1H), 7.50–7.31 (m, 4H), 7.21 (t, J = 7.1 Hz, 1H), 7.11 (t, J = 7.1 Hz, 1H), 6.82 (d, J = 11.0 Hz, 1H), 6.54 (s, 1H), 4.87–4.74 (m, 1H), 3.94 (s, 3H), 3.90 (s, 3H), 3.86 (s, 3H), 3.68 (s, 3H), 2.59–2.50 (m, 1H), 2.46–2.33 (m, 2H), 2.03–1.84 (m, 1H), 1.43 (s, 9H); HRMS (ESI): m/z calcd for $C_{43}H_{43}N_3O_9SNa$ (M + Na^+): 800.2612, found: 800.2606.

4.4. Representative procedure for ***6a–d***

Trifluoroacetic acid (50.0 equiv) was added dropwise into a solution of compound **5a–d** (1.0 equiv) in DCM. The mixture was stirred at room temperature for 3 h and quenched with saturated Na_2CO_3 (aq). Subsequently, the solution was extracted with DCM and the organic layer was dried over Na_2SO_4 and concentrated in vacuo. The crude product was further purified by column chromatography (DCM: MeOH = 20:1).

4.4.1. Compound ***6a***

Starting from acid **5a**, 70% of compound **6a** was obtained as white solid. mp 192–194 °C, ^{1}H NMR (400 MHz, $CDCl_3$) δ 9.32 (s, 1H), 8.50 (d, J = 6.3 Hz, 1H), 7.78 (s, 1H), 7.70 (d, J = 8.0 Hz, 2H), 7.51 (d, J = 7.8 Hz, 2H), 7.37 (d, J = 10.8 Hz, 1H), 7.26–7.23 (m, 1H), 7.00 (t, J = 7.4 Hz, 1H), 6.94 (d, J = 11.0 Hz, 1H), 6.84–6.68 (m, 2H), 6.56 (s, 1H), 4.98–4.83 (m, 1H), 4.02 (s, 3H), 3.92 (s, 3H), 3.90 (s, 3H), 3.55 (s, 3H), 2.61–2.47 (m, 1H), 2.42–2.25 (m, 2H), 2.21–2.09 (m, 1H). HPLC: room temperature; t_R = 9.35 min, UV_{254} = 95.6%; HRMS (ESI): m/z calcd for $C_{34}H_{33}N_3O_7Na$ (M + Na^+): 618.2216, found: 618.2224.

4.4.2. Compound ***6b***

Starting from acid **5b**, 83% of compound **6b** was obtained as pale yellow solid. 191–193 °C, ^{1}H NMR (400 MHz, $CDCl_3$) δ 9.62 (s, 1H), 8.49 (d, J = 5.8 Hz, 1H), 7.80 (d, J = 8.0 Hz, 2H), 7.71 (d, J = 7.8 Hz, 2H), 7.60 (s, 1H), 7.49 (s, 1H), 7.33 (d, J = 10.8 Hz, 1H), 7.20–7.11 (m, 2H), 7.09–7.02 (m, 1H), 7.00–6.94 (m, 1H), 6.88 (d, J = 11.1 Hz, 1H), 6.69 (d, J = 8.2 Hz, 1H), 6.52 (s, 1H), 4.88–4.75 (m, 1H), 4.44 (br s, 2H), 3.98 (s, 3H), 3.90 (s, 6H), 3.62 (s, 3H), 2.53–2.39 (m, 1H), 2.37–2.12 (m, 2H), 2.04–1.88 (m, 1H). HPLC: room temperature; t_R = 10.94 min, UV_{254} = 97.5%; HRMS (ESI): m/z calcd for $C_{34}H_{36}N_3O_7S$ (M + H^+): 678.2268, found: 678.2255.

4.4.3. Compound ***6c***

Starting from acid **5c**, 57% of compound **6c** was obtained as pale yellow solid. 178–180 °C, ^{1}H NMR (400 MHz, $CDCl_3$) δ 9.90 (br s, 1H), 8.71 (d, J = 5.0 Hz, 1H), 8.65 (s, 1H), 7.90–7.79 (m, 2H), 7.49 (s, 1H), 7.33 (d, J = 10.8 Hz, 1H), 7.17–7.07 (m, 2H), 7.03 (t, J = 7.5 Hz, 1H), 6.87–6.75 (m, 2H), 6.71 (t, J = 7.5 Hz, 1H), 6.52 (s, 1H), 4.76–4.67 (m, 1H), 4.59 (br s, 2H), 3.94 (s, 3H), 3.92 (s, 3H), 3.90 (s, 3H), 3.74 (s, 3H), 2.52–2.42 (m, 1H), 2.37–2.25 (m, 1H), 2.21–2.09 (m, 1H), 1.85–1.72 (m, 1H). HPLC: room temperature; t_R = 9.66 min, UV_{254} = 97.0%; HRMS (ESI): m/z calcd for $C_{34}H_{33}N_3O_7Na$ (M + Na^+): 618.2216, found: 618.2247.

4.4.4. Compound ***6d***

Starting from acid **5d**, 60% of compound **6d** was obtained as pale yellow solid. mp 191–192 °C, ^{1}H NMR (400 MHz, $CDCl_3$) δ 9.64 (br s, 1H), 8.80 (br s, 1H), 8.65 (s, 1H), 7.91 (d, J = 7.8 Hz, 1H), 7.83 (d, J = 7.8 Hz, 1H), 7.60 (s, 1H), 7.40 (s, 1H), 7.32–7.27 (m, 2H), 7.19–7.04 (m, 3H), 7.01–6.94 (m, 1H), 6.76 (d, J = 10.0 Hz, 2H), 6.51 (s, 1H), 4.80–4.53 (m, 3H), 3.93 (s, 3H), 3.90 (s, 3H), 3.79 (s, 3H), 3.77 (s, 3H), 2.54–2.29 (m, 2H), 2.26–2.12 (m, 1H), 1.89–1.77 (m, 1H). HPLC: room temperature; t_R = 11.06 min, UV_{254} = 96.5%; HRMS (ESI): m/z calcd for $C_{34}H_{36}N_3O_7S$ (M + H^+): 678.2268, found: 678.2220.

4.5. Representative procedure for ***9a–d***

Acid **7**/**8** (1.0 equiv), $SOCl_2$ (6.0 equiv) and DMF (1 drop) were stirred in toluene at 60 °C for 2 h. Then the solvent was removed

under reduced pressure. The acyl chloride was dissolved in DCM and added dropwise into a solution of corresponding aromatic amine (1.0 equiv) and triethylamine (3.0 equiv). After stirring for 1 h at room temperature, the solution was extracted with EtOAc, washed with 1 N HCl (aq) followed by brine and dried over Na_2SO_4. Concentrated in vacuo gave the crude product, which was further purified by column chromatography.

4.5.1. tert-Butyl (2-(4-(chloromethyl)benzamido)phenyl)carbamate (**9a**)

Starting from acid **7** and tert-butyl (2-aminophenyl)carbamate, 82% of compound **9a** was obtained as white solid. mp 176–177 °C, ^{1}H NMR (400 MHz, $CDCl_3$) δ 9.24 (s, 1H), 7.97 (d, J = 8.1 Hz, 2H), 7.83 (d, J = 7.8 Hz, 1H), 7.49 (d, J = 8.2 Hz, 2H), 7.26–7.14 (m, 3H), 6.73 (s, 1H), 4.64 (s, 2H), 1.52 (s, 9H); HRMS (ESI): m/z calcd for $C_{19}H_{21}ClN_2O_3Na$ ($M + Na^+$): 383.1133, found: 383.1149.

4.5.2. tert-Butyl (2-(4-(chloromethyl)benzamido)-4-(thiophen-2-yl)phenyl)carbamate (**9b**)

Starting from acid **7** and tert-butyl (2-amino-4-(thiophen-2-yl) phenyl)carbamate, 84% of compound **9b** was obtained as pale yellow solid. mp 167–169 °C, ^{1}H NMR (400 MHz, $CDCl_3$) δ 9.23 (br s, 1H), 8.09 (d, J = 1.6 Hz, 1H), 7.98 (d, J = 8.2 Hz, 2H), 7.50 (d, J = 8.2 Hz, 2H), 7.40 (dd, J = 8.3, 2.1 Hz, 1H), 7.31–7.28 (m, 1H), 7.28–7.26 (m, 1H), 7.26–7.23 (m, 1H), 7.06 (dd, J = 5.0, 3.6 Hz, 1H), 6.76 (s, 1H), 4.64 (s, 2H), 1.52 (s, 9H); HRMS (ESI): m/z calcd for $C_{23}H_{23}ClN_2O_3SNa$ ($M + Na^+$): 465.1010, found: 465.1001.

4.5.3. tert-Butyl (2-(3-(chloromethyl)benzamido)phenyl)carbamate (**9c**)

Starting from acid **8** and tert-butyl (2-aminophenyl)carbamate, 95% of compound **9c** was obtained as white solid. mp 50–52 °C, ^{1}H NMR (400 MHz, $CDCl_3$) δ 9.25 (br s, 1H), 7.99 (s, 1H), 7.92 (d, J = 7.8 Hz, 1H), 7.82 (d, J = 7.9 Hz, 1H), 7.59 (d, J = 7.7 Hz, 1H), 7.48 (t, J = 7.7 Hz, 1H), 7.26–7.15 (m, 3H), 6.74 (s, 1H), 4.64 (s, 2H), 1.52 (s, 9H); HRMS (ESI): m/z calcd for $C_{19}H_{21}ClN_2O_3Na$ ($M + Na^+$): 383.1133, found: 383.1129.

4.5.4. tert-Butyl (2-(3-(chloromethyl)benzamido)-4-(thiophen-2-yl)phenyl)carbamate (**9d**)

Starting from acid **8** and tert-butyl (2-amino-4-(thiophen-2-yl) phenyl)carbamate, 94% of compound **9d** was obtained as brown soild. mp 146–148 °C, ^{1}H NMR (400 MHz, $CDCl_3$) δ 9.27 (br s, 1H), 8.07 (d, J = 1.8 Hz, 1H), 8.01 (s, 1H), 7.93 (d, J = 7.8 Hz, 1H), 7.60 (d, J = 7.7 Hz, 1H), 7.48 (t, J = 7.7 Hz, 1H), 7.40 (dd, J = 8.3, 2.1 Hz, 1H), 7.29 (dd, J = 3.6, 1.0 Hz, 1H), 7.26–7.21 (m, 2H), 7.05 (dd, J = 5.1, 3.6 Hz, 1H), 6.80 (s, 1H), 4.64 (s, 2H), 1.52 (s, 9H); HRMS (ESI): m/z calcd for $C_{23}H_{23}ClN_2O_3SNa$ ($M + Na^+$): 465.1010, found: 465.1001.

4.6. Representative procedure for **10a–d**

A mixture of de-Ac-colchicine (1.0 equiv), compound **9a–d** (1.5 equiv), NaOAc (5.0 equiv) and KI (1.2 equiv) were refluxed in THF for 48 h. Then the mixture was cooled to room temperature and extracted with EtOAc. The organic layer was washed with 10% $Na_2S_2O_3$ (aq) followed by brine and dried over Na_2SO_4. Concentrated in vacuo gave the crude product, which was further purified by column chromatography (DCM: MeOH = 20:1).

4.6.1. Compound **10a**

Starting from compound **9a**, 80% of compound **10a** was obtained as pale yellow solid. mp 139–141 °C, ^{1}H NMR (400 MHz, $CDCl_3$) δ 9.10 (s, 1H), 7.89–7.80 (m, 3H), 7.75 (dd, J = 7.8, 1.3 Hz, 1H), 7.36–7.29 (m, 3H), 7.25–7.11 (m, 3H), 6.99 (s, 1H), 6.80 (d, J = 11.0 Hz, 1H), 6.52 (s, 1H), 3.98 (s, 3H), 3.91 (s, 3H), 3.90 (s, 3H), 3.79–3.74 (m, 1H), 3.59 (s, 3H), 3.52–3.43 (m, 2H), 2.53–2.31 (m, 2H), 2.30–2.14 (m, 1H), 1.70–1.65 (m, 1H), 1.50 (s, 9H); HRMS (ESI): m/z calcd for $C_{39}H_{43}N_3NaO_8$ ($M + Na^+$): 704.2942, found: 704.2938.

4.6.2. Compound **10b**

Starting from compound **9b**, 56% of compound **10b** was obtained as pale yellow solid. mp 157–159 °C, ^{1}H NMR (400 MHz, $CDCl_3$) δ 9.01 (br s, 1H), 8.05 (s, 1H), 7.91–7.80 (m, 3H), 7.44–7.29 (m, 6H), 7.25–7.19 (m, 1H), 7.09–7.02 (m, 1H), 6.88 (s, 1H), 6.81 (d, J = 10.8 Hz, 1H), 6.52 (s, 1H), 3.99 (s, 3H), 3.91 (s, 3H), 3.90 (s, 3H), 3.79 (d, J = 13.8 Hz, 1H), 3.60 (s, 3H), 3.51 (d, J = 13.6 Hz, 1H), 3.45 (dd, J = 10.8, 6.2 Hz, 1H), 2.52–2.34 (m, 2H), 2.28–2.17 (m, 1H), 1.78–1.67 (m, 1H), 1.52 (s, 9H) HRMS (ESI): m/z calcd for $C_{43}H_{45}N_3NaO_8S$ ($M + Na^+$): 786.2820, found: 786.2820.

4.6.3. Compound **10c**

Starting from compound **9c**, 88% of compound **10c** was obtained as yellow soild. mp 99–101 °C, ^{1}H NMR (400 MHz, $CDCl_3$) δ 9.08 (br s, 1H), 7.97 (s, 1H), 7.85 (s, 1H), 7.79 (d, J = 7.5 Hz, 2H), 7.44–7.31 (m, 3H), 7.25–7.15 (m, 3H), 7.09 (s, 1H), 6.81 (d, J = 10.7 Hz, 1H), 6.53 (s, 1H), 3.98 (s, 3H), 3.91 (s, 3H), 3.89 (s, 3H), 3.72 (d, J = 13.4 Hz, 1H), 3.60–3.52 (m, 4H), 3.46 (dd, J = 10.8, 6.2 Hz, 1H), 2.52–2.33 (m, 2H), 2.31–2.18 (m, 1H), 1.78–1.72 (m, 1H), 1.47 (s, 9H); HRMS (ESI): m/z calcd for $C_{39}H_{43}N_3NaO_8$ ($M + Na^+$): 704.2942, found: 704.2947.

4.6.4. Compound **10d**

Starting from compound **9d**, 56% of compound **10d** was obtained as yellow soild. mp 146–148 °C, ^{1}H NMR (400 MHz, $CDCl_3$) δ 9.13 (br s, 1H), 8.12–7.99 (m, 2H), 7.91–7.78 (m, 2H), 7.45–7.30 (m, 6H), 7.25–7.14 (m, 2H), 7.10–7.03 (m, 1H), 6.82 (d, J = 10.8 Hz, 1H), 6.53 (s, 1H), 3.97 (s, 3H), 3.91 (s, 3H), 3.89 (s, 3H), 3.71 (d, J = 12.5 Hz, 1H), 3.61 (d, J = 13.3 Hz, 1H), 3.56 (s, 3H), 3.51–3.44 (m, 1H), 2.52–2.33 (m, 2H), 2.31–2.19 (m, 1H), 1.78–1.70 (m, 1H), 1.48 (s, 9H); HRMS (ESI): m/z calcd for $C_{43}H_{45}N_3NaO_8S$ ($M + Na^+$): 786.2820, found: 786.2822.

4.7. Representative procedure for **11a–d**

Trifluoroacetic acid (50.0 equiv) was added dropwise into a solution of compound **10a–d** (1.0 equiv) in DCM. The mixture was stirred for 3 h at room temperature and quenched with saturated Na_2CO_3 (aq). The solution was extracted with DCM and the organic layer was dried over Na_2SO_4 and concentrated in vacuo. The crude product was further purified by column chromatography (DCM: MeOH = 20:1).

4.7.1. Compound **11a**

Starting from compound **10a**, 56% of compound **11a** was obtained as white solid. mp 128–129 °C, ^{1}H NMR (400 MHz, $CDCl_3$) δ 8.04 (s, 1H), 7.83 (s, 1H), 7.76 (d, J = 6.9 Hz, 2H), 7.41–7.29 (m, 3H), 7.23 (d, J = 10.7 Hz, 1H), 7.07 (t, J = 7.4 Hz, 1H), 6.91–6.75 (m, 3H), 6.52 (s, 1H), 3.96 (s, 3H), 3.91 (s, 3H), 3.90 (s, 3H), 3.73 (d, J = 13.5 Hz, 1H), 3.60 (s, 3H), 3.54 (d, J = 13.5 Hz, 1H), 3.47–3.41 (m, 1H), 2.50–2.34 (m, 2H), 2.28–2.15 (m, 1H), 1.77–1.65 (m, 1H). HPLC: room temperature; t_R = 7.89 min, UV_{254} = 100.0%; HRMS (ESI): m/z calcd for $C_{34}H_{35}N_3NaO_6$ ($M + Na^+$): 604.2418, found: 604.2454.

4.7.2. Compound **11b**

Starting from compound **10b**, 57% of compound **11b** was obtained as white solid. mp 143–145 °C, ^{1}H NMR (400 MHz, $CDCl_3$) δ 8.02 (br s, 1H), 7.82 (s, 1H), 7.78 (d, J = 8.1 Hz, 2H), 7.65 (s, 1H), 7.38–7.31 (m, 3H), 7.25–7.16 (m, 3H), 7.02 (dd, J = 4.9, 3.8 Hz, 1H), 6.82 (dd, J = 19.4, 9.5 Hz, 2H), 6.52 (s, 1H), 3.96 (s, 3H), 3.92 (s, 3H), 3.90 (s, 3H), 3.74 (d, J = 13.6 Hz, 1H), 3.61 (s, 3H), 3.57 (d, J = 13.6 Hz, 1H), 3.43 (dd, J = 10.8, 6.2 Hz, 1H), 2.51–2.32 (m, 2H), 2.27–2.16 (m,

1H), 1.75–1.70 (m, 1H). HPLC: room temperature; t_R = 9.85 min, UV_{254} = 95.0%; HRMS (ESI): *m/z* calcd for $C_{38}H_{38}N_3O_6S$ ($M + H^+$): 664.2476, found: 664.2513.

4.7.3. Compound **11c**

Starting from compound **10c**, 38% of compound **11c** was obtained as pale yellow solid. mp 120–122 °C, ^1H NMR (400 MHz, $CDCl_3$) δ 8.36 (br s, 1H), 7.97 (s, 1H), 7.88 (s, 1H), 7.76 (d, J = 6.9 Hz, 1H), 7.44 (d, J = 7.6 Hz, 1H), 7.38–7.28 (m, 2H), 7.25–7.20 (m, 1H), 7.07 (t, J = 7.3 Hz, 1H), 6.91–6.77 (m, 3H), 6.53 (s, 1H), 3.97 (s, 3H), 3.91 (s, 3H), 3.90 (s, 3H), 3.72–3.58 (m, 2H), 3.57 (s, 3H), 3.50–3.43 (m, 1H), 2.51–2.44 (m, 1H), 2.43–2.34 (m, 1H), 2.30–2.22 (m, 1H), 1.78–1.69 (m, 1H). HPLC: room temperature; t_R = 8.09 min, UV_{254} = 95.9%; HRMS (ESI): *m/z* calcd for $C_{34}H_{35}N_3NaO_6$ ($M + Na^+$): 604.2418, found: 604.2464.

4.7.4. Compound **11d**

Starting from compound **10d**, 31% of compound **11d** was obtained as yellow solid. mp 136–138 °C, ^1H NMR (400 MHz, $CDCl_3$) δ 8.46 (br s, 1H), 8.01 (s, 1H), 7.91 (s, 1H), 7.84–7.69 (m, 2H), 7.41–7.30 (m, 3H), 7.26–7.13 (m, 3H), 7.07–6.99 (m, 1H), 6.88–6.75 (m, 2H), 6.54 (s, 1H), 3.96 (s, 3H), 3.92 (s, 3H), 3.90 (s, 3H), 3.71–3.63 (m, 2H), 3.58 (s, 3H), 3.52–3.44 (m, 1H), 2.51–2.34 (m, 2H), 2.31–2.21 (m, 1H), 1.77–1.72 (m, 1H). HPLC: room temperature; t_R = 9.97 min, UV_{254} = 95.0%; HRMS (ESI): *m/z* calcd for $C_{38}H_{38}N_3O_6S$ ($M + H^+$): 664.2476, found: 664.2517.

4.8. HDAC enzymatic assay in vitro

Recombinant human HDAC1, HDAC2 and HDAC3 were cloned and expressed in High5 insect cells using a baculovirus expression system and purified using Ni-NTA (QIAGEN). The histone deacetylase inhibitory activity was determined using the HDAC substrate Ac–Lys–Tyr–Lys (ε-acetyl)-AMC. The reaction was carried out in black 384-well plates (OptiPlateTM-384F, PerkinElmer) at room temperature. The typical inhibition assay was carried out in 25 μL of buffer containing 25 mM HEPES, 137 mM NaCl, 2.7 mM KCl and 4.9 mM $MgCl_2$, pH 8.0, HDAC protein (20–200 nM), HDAC substrate (5–50 μM) and individual compound. Positive controls contained mocetinostat and all the above components except the inhibitor. The negative controls contained neither enzyme nor inhibitor. After incubation for 24 h and 3 h respectively, the reaction of HDAC1, HDAC2 and HDAC3 was quenched with the addition of 25 μL Trypsin (diluted to a final concentration of 0.3125%). After 30 min, the fluorescence generated was monitored at 355 nm (excitation) and 460 nm (emission) using an EnVision multilabel plate reader (PerkinElmer Life Sciences, Boston, MA, USA).

4.9. Cell culture and cytotoxicity/proliferation assay

Cells were kept at logarithmic growth phase in 5% CO_2 at 37 °C with the corresponding medium supplemented with 10% fetal bovine serum and 100 units/mL each of penicillin G and streptomycin. Cells were seeded onto a 96–well plate at a concentration of 2000–3000 cells/well and incubated at 37 °C in 5% CO_2 for 24 h. A range of concentrations of the test compounds were added and the plate was incubated at 37 °C for 72 h before the addition of 20 μL MTT (5 mg/mL)/well. After 3 h of incubation, the medium was removed and 100 μL DMSO was added to each well. The absorbance was measured using a SpectraMax 340 microplate reader (Molecular Devices, Sunnyvale, CA, USA) at 550 nm. The optical density of the result of the MTT assay was directly proportional to the number of viable cells.

4.10. Cell cycle analysis

Cells treated with test compounds for 24 h were collected and cell cycle distribution was determined by flow cytometry. In brief, the cellular DNA content was measured on an easyCyte 6HT-2L (Millipore) after cells were incubated with RNase A (10 mg/mL) and propidium iodide (50 mg/mL). The percentage of each population was analysed using ModFIT software (BD Biosciences). At least 20 000 cells were analyzed for each data point.

Acknowledgments

This work was supported by the grants of National Natural Science Foundation of China (No. 81172936 and No. 81173033).

Appendix A. Supplementary data

Supplementary data related to this article can be found at http://dx.doi.org/10.1016/j.ejmech.2015.03.035.

References

[1] Internaional Agency for Research on Cancer, World Cancer Report 2014, World Health Organization, Geneva, 2014.
[2] L. Costantino, D. Barlocco, Challenges in the design of multitarget drugs against multifactorial pathologies: a new life for medicinal chemistry? Future Med. Chem. 5 (2013) 5–7.
[3] M.S. Kim, M. Blake, J.H. Baek, G. Kohlhagen, Y. Pommier, F. Carrier, Inhibition of histone deacetylase increases cytotoxicity to anticancer drugs targeting DNA, Cancer Res. 63 (2003) 7291–7300.
[4] F. Bruzzese, M. Rocco, S. Castelli, E. Di Gennaro, A. Desideri, A. Budillon, Synergistic antitumor effect between vorinostat and topotecan in small cell lung cancer cells is mediated by generation of reactive oxygen species and DNA damage-induced apoptosis, Mol. Cancer Ther. 8 (2009) 3075–3087.
[5] R.L. Bevins, S.G. Zimmer, It's about time: scheduling alters effect of histone deacetylase inhibitors on camptothecin-treated cells, Cancer Res. 65 (2005) 6957–6966.
[6] M. Ocker, A. Alajati, M. Ganslmayer, S. Zopf, M. Luders, D. Neureiter, E.G. Hahn, D. Schuppan, C. Herold, The histone-deacetylase inhibitor SAHA potentiates proapoptotic effects of 5-fluorouracil and irinotecan in hepatoma cells, J. Cancer Res. Clin. Oncol. 131 (2005) 385–394.
[7] B. Sarcar, S. Kahali, P. Chinnaiyan, Vorinostat enhances the cytotoxic effects of the topoisomerase I inhibitor SN38 in glioblastoma cell lines, J. Neuro-Oncol. 99 (2010) 201–207.
[8] M. Dokmanovic, C. Clarke, P.A. Marks, Histone deacetylase inhibitors: overview and perspectives, Mol. Cancer Res. 5 (2007) 981–989.
[9] H.Y. Lin, C.S. Chen, S.P. Lin, J.R. Weng, C.S. Chen, Targeting histone deacetylase in cancer therapy, Med. Res. Rev. 26 (2006) 397–413.
[10] M.J. Lee, Y.S. Kim, S. Kummar, G. Giaccone, J.B. Trepel, Histone deacetylase inhibitors in cancer therapy, Curr. Opin. Oncol. 20 (2008) 639–649.
[11] C.S. Chen, S.C. Weng, P.H. Tseng, H.P. Lin, C.S. Chen, Histone acetylation-independent effect of histone deacetylase inhibitors on Akt through the reshuffling of protein phosphatase 1 complexes, J. Biol. Chem. 280 (2005) 38879–38887.
[12] K. Nepali, S. Sharma, M. Sharma, P. Bedi, K. Dhar, Rational approaches, design strategies, structure activity relationship and mechanistic insights for anticancer hybrids, Eur. J. Med. Chem. 77 (2014) 422–487.
[13] K.A. Papavassiliou, A.G. Papavassiliou, Histone deacetylases inhibitors: conjugation to other anti-tumour pharmacophores provides novel tools for cancer treatment, Expert Opin. Invest. Drugs (2013) 1–4.
[14] H. Wang, B.W. Dymock, New patented histone deacetylase inhibitors, Expert Opin. Ther. Pat. 19 (2009) 1727–1757.
[15] A. Saito, T. Yamashita, Y. Mariko, Y. Nosaka, K. Tsuchiya, T. Ando, T. Suzuki, T. Tsuruo, O. Nakanishi, A synthetic inhibitor of histone deacetylase, MS-27-275, with marked in vivo antitumor activity against human tumors, Proc. Natl. Acad. Sci. U. S. A. 96 (1999) 4592–4597.
[16] R.D. Glick, S.L. Swendeman, D.C. Coffey, R.A. Rifkind, P.A. Marks, V.M. Richon, M.P. La Quaglia, Hybrid polar histone deacetylase inhibitor induces apoptosis and CD95/CD95 ligand expression in human neuroblastoma, Cancer Res. 59 (1999) 4392–4399.
[17] L.M. Butler, D.B. Agus, H.I. Scher, B. Higgins, A. Rose, C. Cordon-Cardo, H.T. Thaler, R.A. Rifkind, P.A. Marks, V.M. Richon, Suberoylanilide hydroxamic acid, an inhibitor of histone deacetylase, suppresses the growth of prostate cancer cells in vitro and in vivo, Cancer Res. 60 (2000) 5165–5170.
[18] A.K. Oyelere, P.C. Chen, W. Guerrant, S.C. Mwakwari, R. Hood, Y. Zhang, Y. Fan, Non-peptide macrocyclic histone deacetylase inhibitors, J. Med. Chem. 52 (2009) 456–468.
[19] X. Cai, H.X. Zhai, J. Wang, J. Forrester, H. Qu, L. Yin, C.J. Lai, R. Bao, C. Qian,

Discovery of 7-(4-(3-ethynylphenylamino)-7-methoxyquinazolin-6-yloxy)-N-hydroxyheptanamide (CUDc-101) as a potent multi-acting HDAC, EGFR, and HER2 inhibitor for the treatment of cancer, J. Med. Chem. 53 (2010) 2000–2009.
[20] C.J. Lai, R. Bao, X. Tao, J. Wang, R. Atoyan, H. Qu, D.G. Wang, L. Yin, M. Samson, J. Forrester, B. Zifcak, G.X. Xu, S. DellaRocca, H.X. Zhai, X. Cai, W.E. Munger, M. Keegan, C.V. Pepicelli, C. Qian, CUDC-101, a multitargeted inhibitor of histone deacetylase, epidermal growth factor receptor, and human epidermal growth factor receptor 2, exerts potent anticancer activity, Cancer Res. 70 (2010) 3647–3656.
[21] S. Mahboobi, S. Dove, A. Sellmer, M. Winkler, E. Eichhorn, H. Pongratz, T. Ciossek, T. Baer, T. Maier, T. Beckers, Design of chimeric histone deacetylase- and tyrosine kinase-inhibitors: a series of imatinib hybrides as potent inhibitors of wild-type and mutant BCR-ABL, PDGF-Rbeta, and histone deacetylases, J. Med. Chem. 52 (2009) 2265–2279.
[22] S. Mahboobi, A. Sellmer, M. Winkler, E. Eichhorn, H. Pongratz, T. Ciossek, T. Baer, T. Maier, T. Beckers, Novel chimeric histone deacetylase inhibitors: a series of lapatinib hybrides as potent inhibitors of epidermal growth factor receptor (EGFR), human epidermal growth factor receptor 2 (HER2), and histone deacetylase activity, J. Med. Chem. 53 (2010) 8546–8555.
[23] F. Thaler, Current trends in the development of histone deacetylase inhibitors: a review of recent patent applications, Pharm. Pat. Anal. 1 (2012) 75–90.
[24] X. Zhang, M. Su, Y. Chen, J. Li, W. Lu, The design and synthesis of a new class of RTK/HDAC dual-targeted inhibitors, Molecules 18 (2013) 6491–6503.
[25] X. Zhang, J. Zhang, L.J. Tong, Y. Luo, M.B. Su, Y. Zang, J. Li, W. Lu, Y. Chen, The discovery of colchicine-SAHA hybrids as a new class of antitumor agents, Bioorg. Med. Chem. 21 (2013) 3240–3244.
[26] X. Zhang, B. Bao, X. Yu, L. Tong, Y. Luo, Q. Huang, M. Su, L. Sheng, J. Li, H. Zhu, B. Yang, X. Zhang, Y. Chen, W. Lu, The discovery and optimization of novel dual inhibitors of topoisomerase II and histone deacetylase, Bioorg. Med. Chem. 21 (2013) 6981–6995.
[27] B.S. Mann, J.R. Johnson, M.H. Cohen, R. Justice, R. Pazdur, FDA approval summary: vorinostat for treatment of advanced primary cutaneous T-cell lymphoma, Oncologist 12 (2007) 1247–1252.
[28] C. Grant, F. Rahman, R. Piekarz, C. Peer, R. Frye, R.W. Robey, E.R. Gardner, W.D. Figg, S.E. Bates, Romidepsin: a new therapy for cutaneous T-cell lymphoma and a potential therapy for solid tumors, Expert Rev. Anticancer Ther. 10 (2010) 997–1008.
[29] S.C. Mwakwari, V. Patil, W. Guerrant, A.K. Oyelere, Macrocyclic histone deacetylase inhibitors, Curr. Top. Med. Chem. 10 (2010) 1423–1440.
[30] R.M. Poole, Belinostat: first global approval, Drugs 74 (2014) 1543–1554.
[31] M. Paris, M. Porcelloni, M. Binaschi, D. Fattori, Histone deacetylase inhibitors: from bench to clinic, J. Med. Chem. 51 (2008) 1505–1529.
[32] C.H. Arrowsmith, C. Bountra, P.V. Fish, K. Lee, M. Schapira, Epigenetic protein families: a new frontier for drug discovery, Nat. Rev. Drug Discovery 11 (2012) 384–400.
[33] J.H. Kim, E.K. Yoon, H.J. Chung, S.Y. Park, K.M. Hong, C.H. Lee, Y.S. Lee, K. Choi, Y. Yang, K. Kim, I.H. Kim, p53 acetylation enhances Taxol-induced apoptosis in human cancer cells, Apoptosis 18 (2013) 110–120.
[34] N.H. Chobanian, V.L. Greenberg, J.M. Gass, C.P. Desimone, J.R. Van Nagell, S.G. Zimmer, Histone deacetylase inhibitors enhance paclitaxel-induced cell death in ovarian cancer cell lines independent of p53 status, Anticancer Res. 24 (2004) 539–545.
[35] V. Zuco, M. De Cesare, R. Cincinelli, R. Nannei, C. Pisano, N. Zaffaroni, F. Zunino, Synergistic antitumor effects of novel HDAC inhibitors and paclitaxel in vitro and in vivo, PloS One 6 (2011) e29085.
[36] J.D. Bagnato, A.L. Eilers, R.A. Horton, C.B. Grissom, Synthesis and characterization of a cobalamin-colchicine conjugate as a novel tumor-targeted cytotoxin, J. Org. Chem. 69 (2004) 8987–8996.
[37] L. Cosentino, M. Redondo-Horcajo, Y. Zhao, A.R. Santos, K.F. Chowdury, V. Vinader, Q.M. Abdallah, H. Abdel-Rahman, J.r.m. Fournier-Dit-Chabert, S.D. Shnyder, Synthesis and biological evaluation of colchicine B-ring analogues tethered with halogenated benzyl moieties, J. Med. Chem. 55 (2012) 11062–11066.
[38] O.M. Moradei, T.C. Mallais, S. Frechette, I. Paquin, P.E. Tessier, S.M. Leit, M. Fournel, C. Bonfils, M.C. Trachy-Bourget, J.H. Liu, T.P. Yan, A.H. Lu, J. Rahil, J. Wang, S. Lefebvre, Z.M. Li, A.F. Vaisburg, J.M. Besterinan, Novel aminophenyl benzamide-type histone deacetylase inhibitors with enhanced potency and selectivity, J. Med. Chem. 50 (2007) 5543–5546.
[39] M.A. Jordan, L. Wilson, Microtubules as a target for anticancer drugs, Nat. Rev. Cancer 4 (2004) 253–265.